Chinese Journal of Electronics
Vol.32, No.1, Jan. 2023

Non-uniform Compressive Sensing Imaging Based on Image Saliency

LI Hongliang[1,2], DAI Feng[2], ZHAO Qiang[2], MA Yike[2], CAO Juan[2], and ZHANG Yongdong[3]

(1. *University of Chinese Academy of Sciences, Beijing 100049, China*)

(2. *Key Lab of Intelligent Information Processing of Chinese Academy of Sciences, Institute of Computing Technology, Chinese Academy of Sciences, Beijing 100190, China*)

(3. *University of Science and Technology of China, Hefei 230027, China*)

Abstract — For more effective image sampling, compressive sensing (CS) imaging methods based on image saliency have been proposed in recent years. Those methods assign higher measurement rates to salient regions, but lower measurement rate to non-salient regions to improve the performance of CS imaging. However, those methods are block-based, which are difficult to apply to actual CS sampling, as each photodiode should strictly correspond to a block of the scene. In our work, we propose a non-uniform CS imaging method based on image saliency, which assigns higher measurement density to salient regions and lower density to non-salient regions, where measurement density is the number of pixels measured in a unit size. As the dimension of the signal is reduced, the quality of reconstructed image will be improved theoretically, which is confirmed by our experiments. Since the scene is sampled as a whole, our method can be easily applied to actual CS sampling. To verify the feasibility of our approach, we design and implement a hardware sampling system, which can apply our non-uniform sampling method to obtain measurements and reconstruct the images. To our best knowledge, this is the first CS hardware sampling system based on image saliency.

Key words — Compressive sensing, Non-uniform, Measurement density, Image saliency.

I. Introduction

Compressive sensing (CS) is a signal compression theory that can sample and reconstruct a signal at sub-Nyquist sampling rate. The definition of CS was introduced by Candes *et al.* in [1] and [2]. CS can be simply defined as

$$\boldsymbol{y} = \boldsymbol{\Phi x} \tag{1}$$

where $\boldsymbol{x} \in \mathbb{R}^n$ is the signal to be compressed, $\boldsymbol{y} \in \mathbb{R}^m$ is the compressed data, which is usually called measurements. $\boldsymbol{\Phi} \in \mathbb{R}^{m \times n}$ is the measurement matrix. The reconstruction of CS is to recover $\boldsymbol{x}$ by $\boldsymbol{y}$. Since $m \ll n$, the problem is underdetermined, and the rate of m/n can be called measurement rate (MR) or sampling rate. Usually, higher MRs correspond to better reconstruction results. It is obviously that more measurements will get better reconstruction. However, if we reduce the dimension of signal $\boldsymbol{x}$, we can also get better reconstruction.

In CS imaging, one of the main challenges is to reconstruct higher quality images with fewer measurements. To this end, we need more efficient sampling methods and better reconstruction algorithms. Researches show that human perception of image quality is largely influenced by visual attention, and that human vision would pay more attention to salient regions of an image, but less attention to the rest of the image [3]. In recent years, many researchers use the saliency information for more effective CS sampling. Those methods divide the image into blocks and assign different sampling times for different blocks according to the saliency of each block, which means applying a higher measurement rate to a more salient block and a lower measurement rate to a less salient block. However, due to the non-uniform sampling times for different image block, those methods are difficult to apply in a real sampling hardware. As it is mentioned in [4], they need block-wise mega-pixel sensor (BMPS) to do the sampling process. The sensor is actually an array of photodiodes, which needs strict calibration for each photodiode corresponding to a block of the scene.

Manuscript Received Jan. 18, 2019; Accepted May 24, 2019.
 DOI:10.23919/cje.2019.00.028

However, the rays of a scene block are easily disturbed by the rays of adjacent blocks. Therefore, each photodiode cannot accurately capture the rays of each image block. Another way of implementation is to sample a block of image by covering other image blocks. The sampling time of this way will significantly increase, and the sampling process will be much more complicated.

In our work, we propose a non-uniform sampling method based on image saliency. Different from the previous non-uniform sampling in MRs, the method implements non-uniform sampling by assigning different measurement density in different salient regions, where measurement density is the number of pixels to be measured in a unit size. As we analyzed before, a higher MR correspond to a better reconstruction. The block-based CS sampling methods improve the image quality by increasing the numbers of measurements in salient regions, while our method achieves this by reducing the dimensions of less salient regions. As sampling times for different regions are the same, our method can be easily applied into the existing compressive sensing imaging devices. To validate our approach, we design and implement a hardware prototype system that can apply non-uniform sampling method to obtain measurements and reconstruct images. In order to do reconstruction with our measurements, we improve the traditional reconstruction algorithms. Experiments show that the improved algorithms can significantly improve the reconstructed image quality.

II. Related Work

In this section, we will introduce the block-based CS sampling method in detail. Then, we will briefly introduce the reconstruction algorithm in order to understand our improved reconstruction algorithm. And also several sampling hardware system will be introduced to help understand our sampling system.

1. Block based CS sampling

Traditional CS sampling is done as (1). The image $\boldsymbol{x}$ is sampled by measurement matrix $\boldsymbol{\Phi}$ uniformly. In recent years, many researchers use the saliency information for more effective CS sampling. Yu *et al.* first introduced image saliency into CS sampling in [4]. It proposed a block-based CS sampling scheme that assigned higher MRs to salient image blocks and lower MRs to non-salient image blocks. The size of block is 16×16 pixels, and the image is divided uniformly. This method reconstructed better results in the salient blocks for the higher MRs and the quality of whole image was improved. In order to better estimate the compressibility of the image block, Zhang *et al.* proposed a standard deviation based method to do the estimation from CS measurements [5]. The method firstly got the compressibility of image blocks by a uniform MRs sampling. Then, based on the estimation, the method performed a non-uniform MRs block-based CS sampling. Finally, the method combined twice-sampling data to get better reconstruction results. For the block evaluation method, Li *et al.* proposed an evaluation method based on spatial entropy in [6]. For the block division method, Zhou *et al.* proposed a non-uniform division method based on k-means clustering instead of uniform division. And there are also some block based applications [7], [8]. In any case, those methods are all block based, which are difficult to apply to actual sampling.

2. Reconstruction algorithm

For CS reconstruction, traditional algorithms assume the signal is sparse in some transform domain. Based on this, the problem can be solved by some optimization algorithms, such as gradient projection for sparse reconstruction (GPSR) [9], iterative shrinkage thresholding [10], total variation [11], greedy [12], low-rank [13], etc. In recent years, several algorithms based on image structure features have been proposed, such as TVAL3 [14] and DAMP [15]. They assume that natural image signal is structure-sparsity. Inspired by deep neural network (DNN), Metzler *et al.* extend the work of DAMP and propose an algorithm LDAMP [16] combining traditional algorithm and DNN algorithm.

Regardless of the assumptions, the reconstruction algorithm needs to iterate continuously under the constraints of $\boldsymbol{y} = \boldsymbol{\Phi x}$. In the iteration process, the transformation between $\boldsymbol{y}$ and $\boldsymbol{x}$ will be carried out continuously, and then the image $\boldsymbol{x}$ will be constrained according to different sparse assumptions mentioned above in each iteration. By iterating over and over again, we can finally get the reconstructed image.

3. Sampling in reality

All along, how to apply CS to practice is an important research direction. In the CS sampling hardware, the light of the scene is modulated by the way of (1) and then sampled by a photodiode. The main difficulty is to find a method of light modulation. Reference [17] proposed a single-pixel camera (SPC) for CS, which applied digital micromirror device (DMD) to modulate the light of scene. While Huang *et al.* proposed a lensless CS imaging device in [18], which applied liquid crystal display (LCD) for the modulation. Zhang *et al.* uses a projector to project the measurement matrix into the scene, and then collects the light of the scene [19]. Although the light of the scene is limited by projector, the method is capable of capturing a scene without a direct view of it.

III. Non-uniform CS Imaging

In this section, we begin with introducing the non-uniform sampling method we proposed in detail, and

then describe the improvement in reconstruction algorithm for our non-uniform measurements.

1. Non-uniform sampling

Our non-uniform sampling process is shown in Fig.1. Firstly, we get the saliency map of the image by saliency detection algorithms and quantify the saliency of the pixels to L levels with level L as the most salient regions and level 1 as the least salient regions. In order to reduce the dimension of image, we assign higher measurement density to more salient regions and lower measurement density to less salient regions. This is achieved by assigning smaller sampling units to the more salient regions and bigger sampling unit to less salient regions.

A sampling unit is a square of pixels in which we only sample one pixel. Formally, we assume the width and height of sampling unit are w_l and h_l for level l. In theory, w_l and h_l can be any positive integer. For the higher levels can be divided exactly, we set them to satisfy the following geometric progression.

$$w_l = p^{L-l}, \quad h_l = q^{L-l}, \quad l \in 1, \ldots, L \tag{2}$$

where p and q are the common ratio. In our work, we assume $p = q$. In actual division, the quantified saliency map cannot exactly conform the edge of sampling unit. In that case, we assign the sampling units that contain higher level pixels to higher level sampling units. For our division, we first divide the whole saliency map into sampling unit by the first level of w_1 and h_1. Then we divide the sampling units containing the second level pixels by w_2 and h_2. The third level sampling units are generated by divide all lower level sampling units contain third level pixels, i.e. level 1 and level 2 sampling units. Repeat this process until level L, we will get the non-uniform division in Fig.1. A simple example of this division can be found in Fig.2 and the process of this non-uniform division can be found in Algorithm 1.

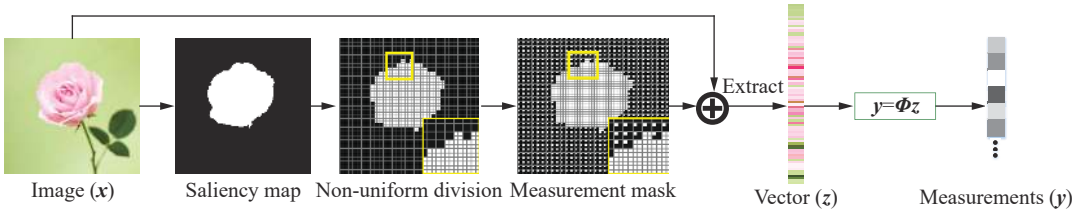

Fig. 1. A simple schematic of non-uniform sampling. Firstly, we get the saliency map from the image by some saliency detection algorithms such as GMR [20]. Then we get the non-uniform division, the each sampling unit of which corresponds to a measurement point. After allocate the measurement point, we get measurement mask. The pixels to be measured are combined to a vector $\boldsymbol{z}$, which are extracted from the image by measurement mask. Finally, the measurements are generated by $\boldsymbol{y} = \boldsymbol{\Phi z}$.

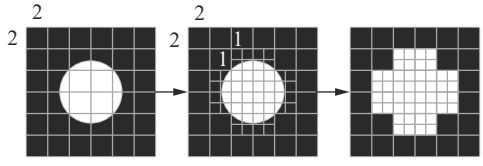

Fig. 2. The process of non-uniform division. We assume the white region of the saliency map has a higher saliency level. Firstly, we divide the whole saliency map into sampling unit by the first level, which is $w_1$and h_1 in the figure, and the result is shown in the left figure. Then we divide the sampling unit containing the second level pixels, which also contains the edge-pixels, and the division is shown in middle figure. The final division is shown in right figure.

For each sampling unit, the sampled pixel called measurement point, and the measurement point can be any pixel in the unit or the average value of all pixels. In our work, we place the measurement point in the upper left corner of the unit. After all of those processes, we will get the measurement mask in Fig.1, which is a mask for the sampling pixels of the image. The pixels of the image $\boldsymbol{x}$ are extracted by the measurement mask to get the pixels $\boldsymbol{z}$, which are no longer a two-dimensional image but a vector. Finally, the vector $\boldsymbol{z}$ is measured by $\boldsymbol{y} = \boldsymbol{\Phi z}$ to get the measurements, which are our non-uniform measurements.

Algorithm 1 The non-uniform division method

Input: w_l and h_l: the size of sampling unit for each level; S_0: saliency map with L level.
Output: S_L: non-uniform division of saliency map.
Initialize: $l \leftarrow 1$;
for l in $\{1, 2, \ldots, L\}$;
  $w_l \leftarrow p^{L-l}$;
  $h_l \leftarrow q^{L-l}$;
  Divide the pixels $\geq$ level l in S_{l-1} by $w_l \times h_l$;
  $S_l \leftarrow$ update pixels of level l;
  for i in $\{l-1, l-2, \ldots, 1\}$;
    Devide level i sampling units contain pixels of level l;
    $S_l \leftarrow$ update pixels of level l;
  end for
end for

2. Algorithm improvement

For our previous sampling, we assume the sampled

pixels of image $\boldsymbol{x}$ are $\boldsymbol{z}$, and the measurements are generated as follows:

$$\boldsymbol{y} = \boldsymbol{\Phi z}, \quad \boldsymbol{z} = E(\boldsymbol{x}, \boldsymbol{m}) \tag{3}$$

where $E(\cdot)$ denotes the process of extracting the pixels of $\boldsymbol{x}$ by the measurement mask $\boldsymbol{m}$. The problem is how to reconstruct $\boldsymbol{x}$ by $\boldsymbol{y}$. The most intuitive way is reconstructing $\boldsymbol{z}$ by traditional reconstruction algorithms, and then up-sampling $\boldsymbol{z}$ to $\boldsymbol{x}$ by the inverse process of $E(\cdot)$. However, we know that $\boldsymbol{z}$ is a pixel vector, which no longer has the structural information of the two-dimensional image. Some recent researches show that using the structural information of image can achieve better reconstruction results in the optimization [14], [15]. To this end, we propose an improved algorithm that allows traditional reconstruction algorithms to reconstruct images using non-uniform measurements.

The iterative-based CS reconstruction algorithm needs to continuously transform between image and measurements to obtain the reconstructed image. Usually we define the transformation of image to measurements as forward transformation and the transformation of measurements to image as inverse transformation. The forward transformation in traditional CS reconstruction algorithm is realized by $\boldsymbol{y} = \boldsymbol{\Phi x}$, and the inverse transformation is realized by $\boldsymbol{x} = \boldsymbol{\Phi}^{\mathrm{T}}\boldsymbol{y}$. Different from the method of directly reconstructing $\boldsymbol{z}$, we add the transformation of $\boldsymbol{x}$ to $\boldsymbol{z}$ before the forward transformation of each iteration, and add transformation of $\boldsymbol{z}$ to $\boldsymbol{x}$ after the inverse transformation of each iteration. A simple schematic of this improvement can be found in Fig.3 , where the iterative optimization refers to the other constraints proposed by reconstruction algorithms, such as TV-normal or denoiser. These iterative optimizations can further improve the image quality, but their inputs are assumed to be two-dimensional images. As our improvement of the algorithm satisfies this assumption, this improvement enables the reconstruction algorithm to utilize non-uniform measurements to optimize two-dimensional images without changing the algorithm flow.

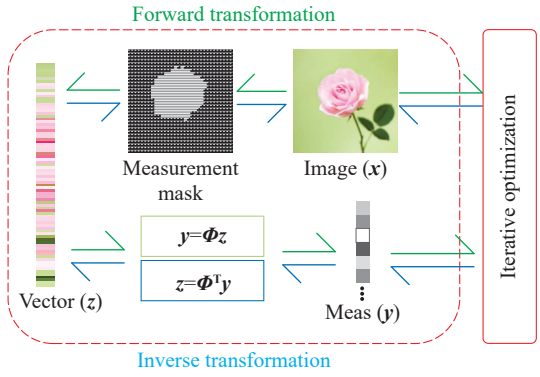

Fig. 3. A simple schematic of reconstruction algorithm for non-uniform measurements. Usually the reconstruction algorithm consists of forward transformation, inverse transformation and iterative optimization. We add the transformation of the image $\boldsymbol{x}$ to the sampled pixels $\boldsymbol{z}$ in the forward transformation and the sampled pixels $\boldsymbol{z}$ to the image $\boldsymbol{x}$ in the inverse transformation, allowing traditional reconstruction algorithms to reconstruct the images using non-uniform measurements.

IV. Experimental Results

We have done plenty of experiments to verify our method, including the use of non-uniform sampling to reconstruct images on variety of algorithms and the impact of improved algorithm on image quality.

1. Reconstruction results

In order to verify our method, we compare the reconstruction results of uniform sampling and non-uniform sampling by the same reconstruction algorithms at the same MRs. Since our method does not depend on any reconstruction algorithms, we choose several state-of-the-art CS reconstruction algorithms, e.g., TVAL3 [14], DAMP [15], and LDAMP [16]. Since the salient regions of the image are usually used for image recognition [21], we choose the image recognition algorithm to evaluate the quality of the reconstructed images as the work [22]. In our work, we use ResNet [23] to calculate the recognition accuracy. We choose ImageNet 2015 [24] as our test set, and the image size is 256×256 pixels. The saliency map is generated by a saliency detection algorithm GMR [20]. The saliency map is quantified into two levels: salient region and non-salient region. We apply $p = q = 4$ for (2). We sample and reconstruct the images using our method at different MRs. The results are shown in Table 1 , and the best results are highlighted. Some visual images are shown in Fig.4. We also compare the PSNR and SSIM for salient regions of the images, and the results can be found in Fig.5. We can find that our method can achieve better results in both traditional algorithms and DNN based algorithms. Our method can get better details in the salient regions of images. Since the reconstruction quality of LDAMP at $MR = 0.2$ is too low, the accuracy of it has no sense, and the same is true for the PSNR and SSIM in Fig.5.

Even if other saliency based compressive sensing methods cannot be implemented on the hardware, we also compared the reconstruction results of other saliency based compressive sensing method, such as SBCS [4]. The results can be found in Table 2. We can find that our method can achieve better reconstruction quality.

2. Algorithm improvement

In our work, we described our improvement in CS

Table 1. Image recognition accuracy by ResNet [23] (The best performance in each cell is highlighted. We can find that our non-uniform sampling method can achieve better result, especially in higher MRs.)

		TVAL3		DAMP		LDAMP	
	MRs	U	NU	U	NU	U	NU
Top-1	0.2	0.14	**0.26**	0.14	**0.29**	**0.04**	0.01
	0.5	0.32	**0.38**	0.28	**0.42**	0.35	**0.40**
	0.8	0.50	**0.56**	0.54	**0.62**	0.56	**0.58**
Top-5	0.2	0.29	**0.48**	0.33	**0.47**	**0.07**	0.02
	0.5	0.55	**0.60**	0.51	**0.63**	0.52	**0.59**
	0.8	0.79	**0.81**	0.75	**0.83**	0.74	**0.76**

Note: "U" means uniform sampling and "NU" indicates non-uniform sampling; "MRs" means the measurement rates; "Top-N" is the accuracy that one of the first N answers given by the image recognition algorithm is correct.

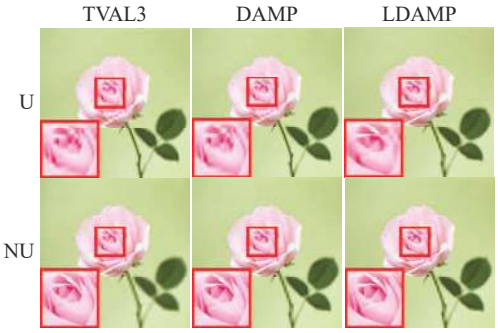

Fig. 4. Images reconstructed by TVAL3, DAMP and LDAMP in $MR = 0.8$. It is obvious that our method has better details in salient region.

reconstruction algorithm. We add the transformation of $\boldsymbol{x}$ to $\boldsymbol{z}$ before the forward transformation of each iteration, and add transformation of $\boldsymbol{z}$ to $\boldsymbol{x}$ after the inverse transformation of each iteration. This improvement can significantly improve the quality of reconstructed images. We perform our non-uniform sampling on the saliency detection data set ECSSD [25], which has an accurate saliency map set. After obtaining the measurements, we reconstruct the image by original reconstruction algorithms and improved algorithms respectively. The reconstructed results are shown in Table 3 and Fig.6. As the DNN based algorithm LDAMP cannot reconstruct one dimensional signal, we do not show the results of LDAMP. We can find that the improved algorithms are able to achieve better PSNR and SSIM at various MRs. At the same time, the improved algorithms can achieve better reconstruction quality in non-salient regions. This will make the image more holistic.

V. Hardware Sampling

To verify the feasibility of our method, we design and implement a real hardware CS imaging system. Due to the need of simultaneously acquire the saliency map and sample the scene, we use the digital micromirror device (DMD) as our spatial light modulator, which

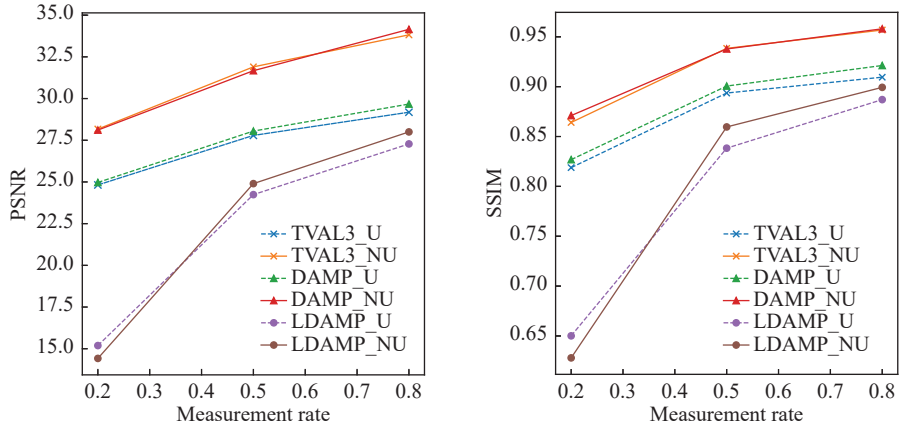

Fig. 5. The PSNR and SSIM for salient regions. Our non-uniform sampling method can get better image quality in salient regions.

Table 2. Reconstructed results (PSNR) of SBCS [4] and ours

MRs	TVAL3		DAMP	
	SBCS	Ours	SBCS	Ours
0.2	20.41	**21.29**	13.82	**21.07**
0.5	22.07	**23.65**	18.49	**24.22**
0.8	23.19	**25.09**	21.23	**25.73**

Table 3. Reconstructed results of the original and improved algorithms (The algorithms with * denote the improved algorithms. Since LDAMP cannot reconstruct one dimension image, we do not show it. We can find that the improved algorithms can significantly improve the quality of reconstructed images, especially in higher MRs)

MRs		TVAL3	TVAL3*	DAMP	DAMP*
0.2	PSNR	21.01	**21.29**	20.81	**21.07**
	SSIM	0.4676	**0.4922**	0.4672	**0.5071**
0.5	PSNR	23.57	**23.65**	23.00	**24.22**
	SSIM	0.5765	**0.5847**	0.5569	**0.6141**
0.8	PSNR	24.91	**25.09**	24.42	**25.73**
	SSIM	0.6354	**0.6424**	0.6157	**0.6703**

Fig. 6. The results of improved reconstruction algorithm in $MR = 0.8$. (a) The original image; (b) The image reconstructed by original algorithm; (c) The image reconstructed by improved algorithm. Since the global optimization of the two-dimensional image, the improved algorithm also get better quality in the non-salient regions of the image.

has bidirectional reflection characteristics. One of the reflected light is captured by a low resolution CMOS (64×64) for obtaining a saliency map of the scene. The other reflected light is collected by a photodiode for obtaining CS measurements. The resolution of DMD is 1920×1080 pixels and we only use 256×256 pixels of the central region. In actual acquisition, the low-resolution CMOS first obtains a low-resolution image to generate a saliency map of the current scene. Since the scene cannot be extracted to a vector as z in hardware, we need to transform the measurement matrix to matrix patterns. The generation of matrix patterns is shown in Fig.7. We rearrange the elements of measurement matrix by the position of measurement points in measurement mask to get the patterns. In our work, we apply Hadamard matrix as our measurement matrix. The matrix patterns are displayed on the DMD, and the measurements are acquired by a photodiode. The optical path diagram and hardware system are shown in Fig.8. The rays of scene are imaged by lens in the plane of DMD. Then the rays reflected by DMD are sampled

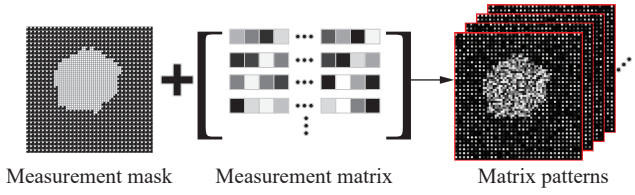

Fig. 7. The generation of matrix patterns. The elements of measurement matrix are rearranged by the position of measurement point in measurement mask to get the matrix patterns.

by CMOS and photodiode with two lenses. The reconstructed results are shown in Fig.9. Our method has clearer details in the image salient regions.

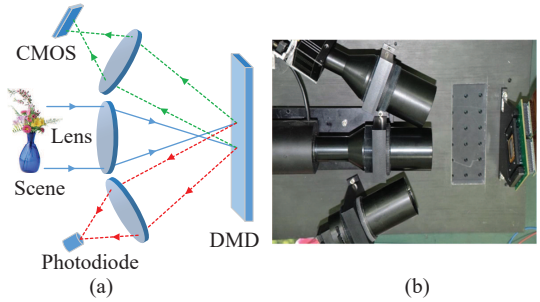

Fig. 8. The optical path of our CS sampling system. (a) is the optical path and (b) is the hardware implementation. The light of scene is imaged on the DMD through lens, and the DMD can reflect light in both directions of ±12 degrees. Thus CMOS and photodiode can receive image of the same viewing angle, CMOS image is used to generate saliency map, and photodiode is used to acquire CS measurements.

Fig. 9. Hardware sampling reconstruction results. The MR for this scene is 0.5. (a) is the scene, (b) is the reconstructed result by uniform sampling, and (c) is the reconstructed result by non-uniform sampling. The image of non-uniform sampling is clearer in the salient region.

VI. Conclusions and Future Work

In conclusion, reducing measurements and improving the quality of image reconstructed have always been challenges for CS imaging. In our work, we propose a non-uniform sampling method. The method utilizes the saliency map of the image to set higher density measurement points in more salient regions and lower density measurement points in less salient regions to reduce the dimension of signal x. For these non-uniform measurements, we design an improved method of CS reconstruction algorithms. This method adds a process of

non-uniform sampling in the process of forward and inverse transformation, respectively, so that the algorithms can optimize the two-dimensional image. Finally, in order to verify the feasibility of our method, we design and implement a hardware system. The experiments show that the non-uniform sampling method can effectively improve the quality of image and increase the recognition accuracy. The optimized algorithm can achieve better quality in non-salient regions. Our method can be applied into a CS hardware sampling system and get a better result. To our best knowledge, this is the first CS hardware sampling system based on image saliency. In the future, we will focus on how to get the saliency evaluation without the low resolution CMOS, which will make the sampling hardware and the light path more simple.

References

[1] E. J. Candès, J. Romberg, and T. Tao, " Robust uncertainty principles: Exact signal reconstruction from highly incomplete frequency information," *IEEE Transactions on Information Theory*, vol.52, no.2, pp.489–509, 2006.

[2] E. J. Candès and M. B. Wakin, " An introduction to compressive sampling," *IEEE Signal Processing Magazine*, vol.25, no.2, pp.21–30, 2008.

[3] A. K. Moorthy and A. C. Bovik, " Visual importance pooling for image quality assessment," *IEEE J. Sel. Top. Sign. Proces.*, vol.3, no.2, pp.193–201, 2009.

[4] Y. Yu, B. Wang, and L. Zhang, " Saliency-based compressive sampling for image signals," *IEEE Signal Processing Letters*, vol.17, no.11, pp.973–976, 2010.

[5] X. Zhang, J. Chen, H. Meng, and X. Tian, "Selfadaptive structured image sensing," *Optical Engineering* , vol.51, no.12, article no.127001, 2012.

[6] R. Li, X. Duan, X. Guo, W. He, and Y. Lv, "Adaptive compressive sensing of images using spatial entropy," *Computational Intelligence and Neuroscience*, vol.2017, pp.1–9, 2017.

[7] B. Zhang, Y. Liu, X. Jing, *et al.*, " Interweaving permutation meets block compressed sensing," *Chinese Journal of Electronics*, vol.27, no.5, pp.1056–1062, 2018.

[8] Z. Li, J. Xie, G. Zhu, *et al.*, "Block-based projection matrix design for compressed sensing," *Chinese Journal of Electronics*, vol.25, no.3, pp.551–555, 2016.

[9] M. A. Figueiredo, R. D. Nowak, and S. J. Wright, "Gradient projection for sparse reconstruction: Application to compressed sensing and other inverse problems," *IEEE Journal of Selected Topics in Signal Processing*, vol.1, no.4, pp.586–597, 2007.

[10] I. Daubechies, M. Defrise, and C. De Mol, " An iterative thresholding algorithm for linear inverse problems with a sparsity constraint," *Communications on Pure and Applied Mathematics*, vol.57, no.11, pp.1413–1457, 2004.

[11] L. I. Rudin, S. Osher, and E. Fatemi, "Nonlinear total variation based noise removal algorithms," *Physica D: Nonlinear Phenomena*, vol.60, no.1-4, pp.259–268, 1992.

[12] L. Jia, "Joint bayesian and greedy recovery for compressive sensing," *Chinese Journal of Electronics*, vol.29, no.5, pp.945–951, 2020.

[13] N. He, R. Wang, J. Lyu, and J. Xue, "Low-rank combined adaptive sparsifying transform for blind compressed sensing image recovery," *Chinese Journal of Electronics* , vol.29, no.4, pp.678–685, 2020.

[14] C. Li, W. Yin, H. Jiang, and Y. Zhang, " An efficient augmented lagrangian method with applications to total variation minimization," *Computational Optimization and Applications*, vol.56, no.3, pp.507–530, 2013.

[15] C. A. Metzler, A. Maleki, and R. G. Baraniuk, " From denoising to compressed sensing," *IEEE Transactions on Information Theory*, vol.62, no.9, pp.5117–5144, 2016.

[16] C. Metzler, A. Mousavi, and R. Baraniuk, " Learned D-AMP: Principled neural network based compressive image recovery," in *Proc. of the 31st Int. Conf. on Neural Information Processing Systems*, Long Beach, CA, USA, pp.1770–1781, 2017.

[17] M. F. Duarte, M. A. Davenport, D. Takhar, *et al.*, "Single-pixel imaging via compressive sampling," *IEEE Signal Processing Magazine*, vol.25, no.2, pp.83–91, 2008.

[18] G. Huang, H. Jiang, K. Matthews, *et al.*, "Lensless imaging by compressive sensing," in *Proceedings of 2013 20th IEEE International Conference on Image Processing (ICIP)*, Melbourne, VIC, Australia, pp.2101–2105, 2013.

[19] Z. Zhang, X. Ma, and J. Zhong, " Single-pixel imaging by means of fourier spectrum acquisition," *Nature Communications*, vol.6, no.1, article no.6225, 2015.

[20] C. Yang, L. Zhang, H. Lu, *et al.*, " Saliency detection via graph-based manifold ranking," in *Proceedings of the IEEE Conference on Computer Vision and Pattern Recognition*, Portland, OR, USA, pp.3166–3173, 2013.

[21] D. Gao, S. Han, and N. Vasconcelos, "Discriminant saliency, the detection of suspicious coincidences. and applications to visual recognition," *IEEE Trans. on Pattern Analysis and Machine Intelligence*, vol.31, no.6, pp.989–1005, 2009.

[22] L. Galteri, L. Seidenari, M. Bertini, *et al.*, "Deep generative adversarial compression artifact removal," in *Proceedings of 2017 IEEE International Conference on Computer Vision (ICCV)*,Venice, Italy, pp.4836–4845, 2017.

[23] K. He, X. Zhang, S. Ren, and J. Sun, "Deep residual learning for image recognition," in *Proceedings of the IEEE Conference on Computer Vision and Pattern Recognition*, Las Vegas, NV, USA, pp.770–778, 2016.

[24] O. Russakovsky, J. Deng, H. Su, *et al.*, " Imagenet large scale visual recognition challenge," *International Journal of Computer Vision*, vol.115, no.3, pp.211–252, 2015.

[25] J. Shi, Q. Yan, L. Xu, *et al.*, " Hierarchical image saliency detection on extended CSSD," *IEEE Trans. on Pattern Analysis and Machine Intelligence*, vol.38, no.4, pp.717–729, 2016.

LI Hongliang reveived the B.S. degree in computer science and technology from the Xidian University, China, in 2011, and the M.S. degree in the Institute of Computing Technology, Chinese Academy of Sciences (CAS), in 2014. He is currently pursuing the Ph.D. degree with the Institute of Computing Technology, CAS. His current research interests include the compressive sensing, computational imaging, machine learning, and neural network. (Email: lihongliang@ict.ac.cn)

DAI Feng (corresponding author) received the Ph.D. degree in the Institute of Computing Technology, CAS, Beijing, China, in 2008. He is currently working as an Associate Professor in the Multimedia Computing Group, Advanced Research Lab, Institute of Computing Technology, CAS. His research interests include image/video processing, computational imaging, and computer vision.
(Email: fdai@ict.ac.cn)